



Gene transfer of two entry inhibitors protects CD4+ T cell from HIV-1 infection in humanized mice

N y Petit, C Baillou, A Burlion, K Dorgham, B Levacher, C Amiel, V Schneider, F M Lemoine, G Gorochoy, Gilles Marodon

► To cite this version:

N y Petit, C Baillou, A Burlion, K Dorgham, B Levacher, et al.. Gene transfer of two entry inhibitors protects CD4+ T cell from HIV-1 infection in humanized mice. *Gene Therapy*, 2015, 23 (2), pp.144-150. 10.1038/gt.2015.101 . hal-01289168

HAL Id: hal-01289168

<https://hal.sorbonne-universite.fr/hal-01289168>

Submitted on 16 Mar 2016

HAL is a multi-disciplinary open access archive for the deposit and dissemination of scientific research documents, whether they are published or not. The documents may come from teaching and research institutions in France or abroad, or from public or private research centers.

L'archive ouverte pluridisciplinaire **HAL**, est destinée au dépôt et à la diffusion de documents scientifiques de niveau recherche, publiés ou non, émanant des établissements d'enseignement et de recherche français ou étrangers, des laboratoires publics ou privés.

Gene transfer of two entry inhibitors protects CD4⁺ T cell from HIV-1 infection in humanized mice

- Running title: HIV-1 gene therapy in humanized mice

Nicolas Y. Petit¹, Claude Baillou¹, Aude Burlion¹, Karim Dorgham¹, Béatrice Levacher², Corinne Amiel^{1,3}, Véronique Schneider³, François M. Lemoine¹, Guy Gorochov^{1,4}, Gilles Marodon¹

¹ Sorbonne Universités, UPMC Univ PARIS 06, CR7, INSERM U1135, CNRS, Centre d'Immunologie et des Maladies Infectieuses (CIMI), Paris, France

² Sorbonne Universités, UPMC Univ PARIS 06, CR7, INSERM U959, Paris, France

³ AP-HP, Hôpital Tenon, Service de Virologie, Paris, France

⁴ AP-HP, Hôpital Pitié-Salpêtrière, Département d'Immunologie, Paris, France

- The authors declare no conflict of interest.

- Corresponding author address: CIMI-PARIS, Bât CERVI, Hôpital Universitaire Pitié-Salpêtrière, 83 Bd de l'Hôpital, 75013 PARIS, FRANCE, tel:+33 1 42 17 7468 Fax: +33 1 42 17 7462, email: gilles.marodon@upmc.fr

This work was supported by grants from Agence Nationale de la Recherche to Guy Gorochov and Gilles Marodon. Nicolas Petit was supported by a doctoral fellowship from Fond Pierre Bergé /SIDAction and by the ANRS.

Abstract

Targeting viral entry is the most likely gene therapy strategy to succeed in protecting the immune system from pathogenic HIV-1 infection. Here, we evaluated the efficacy of a gene transfer lentiviral vector expressing a combination of viral entry inhibitors, the C46 peptide (an inhibitor of viral fusion) and the P2-CCL5 intrakine (a modulator of CCR5 expression), to prevent CD4⁺ T cell depletion *in vivo*. For this, we used two different models of HIV-1-infected mice, one in which *ex vivo* genetically-modified human T cells were grafted into immunodeficient NOD.SCID. γ c^{-/-} mice before infection and one in which genetically-modified T cells were derived from CD34⁺ hematopoietic progenitors grafted few days after birth. Expression of the transgenes conferred a major selective advantage to genetically-modified CD4⁺ T cells, the frequency of which could increase from 10 to 90% in the blood following HIV-1 infection. Moreover, these cells resisted HIV-1-induced depletion, contrary to non-modified cells that were depleted in the same mice. Finally, we report lower normalized viral loads in mice having received genetically-modified progenitors. Altogether, our study documents that targeting viral entry *in vivo* is a promising avenue for the future of HIV-1 gene therapy in humans.

Introduction

Although there is no consensus on a definitive immune correlate of protection, there are multiple convincing examples linking human genetics and susceptibility to HIV-1 infection. The best example of a genetic predisposition protecting from HIV-1 remains the $\Delta 32$ mutation that prevents CCR5 expression at the cell surface, and thus completely protects 1% of Europeans from being infected.¹ The so-called 'Berlin patient' was grafted with CCR5-deficient bone marrow to treat his leukemia and was subsequently cured of both diseases.³ Simultaneously, genetic interventions targeting chemokine receptors using DNA -nucleases gave encouraging results in humanized mice (HuMice)³⁻⁵ but the long term impact of this procedure, as well as the concerns with off-target cleavages, is still unknown. Clinical trials applying this strategy to lymphocytes or stem cells have shown that modified cells possessed a selective advantage compared with non-modified cells,⁶ which is one criterion of success for the therapy. Thus, there is a strong rationale to use gene therapy as an adjunct to current and future treatments.⁷

Maraviroc, a CCR5 chemical antagonist, is a powerful medication *in vitro* but resistant variants rapidly emerge in treated patients for complex reasons, such as mutations in the gp120 coding sequence affecting CCR5 docking.⁸ Similarly, the fusion inhibitor Enfuvirtide (a gp41 analog), which is delivered in solution to patients, rapidly becomes ineffective because gp41 mutates to escape Enfuvirtide binding.⁹ Thus, the therapeutic arsenal targeting viral entry is scarce and poorly efficient. However, strategies based on blocking entry are perhaps the most promising to rapidly restore a pool of functional T cells, the main goal to prevent AIDS.¹⁰ More recently, it was shown that HIV-1 infection needs not to be productive in CD4⁺ T cells to induce

59 cell death by pyroptosis ¹¹. This mechanism of HIV-1-induced cell death highlights the interest of
60 strategies aimed at preventing viral entry. We proposed developing a gene transfer vector in
61 which two viral entry inhibitors in combination would have a better efficacy at preventing viral
62 entry. In support of this hypothesis, a synergistic effect of Enfuvirtide was demonstrated in cells
63 with low levels of CCR5 ¹². Importantly, viral variants able to escape gp41 analogs and CCR5
64 inhibitors at the same time have only been described *in vitro* with a drastic cost on viral fitness, ¹³
65 illustrating the difficulty for the virus to escape both inhibitors at the same time. Using
66 monocistronic lentiviral vectors, we previously showed a synergistic effect of the P2-CCL5
67 intrakine with the C46 peptide on HIV-1 infection *in vitro* ¹⁴. The P2-CCL5 intrakine, originally
68 described as a high affinity CCL5 (RANTES) variant, ¹⁵ was later modified to incorporate an ER
69 retention sequence, sequestering CCR5 away from the cell surface ¹⁶. The C46 peptide is the
70 optimized membrane-bound form of Enfuvirtide and has been used in several gene therapy
71 studies since it is effective on both CCR5- or CXCR4-tropic HIV-1, and can be accommodated in
72 several gene transfer vectors, including lentiviral vectors ¹⁷⁻²⁰. Here, we aimed to evaluate the *in*
73 *vivo* efficacy of an optimized lentiviral vector co-expressing those two entry inhibitors. We used
74 two pre-clinical models of HIV-1 gene therapy, either infusing genetically-modified T cells in
75 adult immunocompromised NOD.SCID.gc^{-/-} (NSG/PBL) mice or grafting genetically-modified
76 hematopoietic progenitors in NSG neonates (NSG/CD34).

Results

A lentiviral vector expressing two inhibitors of HIV-1 entry

With the general aim to validate the combination of the C46 peptide and the P2-CCL5 intrakine for HIV-1 gene therapy *in vivo*, we used an optimized version of our previously described lentiviral vector, which efficiently inhibited HIV-1 infection *in vitro*.¹⁴ To facilitate detection of genetically-modified cells, we added the GFP reporter gene after the therapeutic cassette to generate the LvGFP-C46-P2 vector (Fig. 1a). A vector using the same strong promoter EF1 α but in which the therapeutic cassette was omitted was used as a control (Fig. 1a). We transduced anti-CD3/CD28 activated PBMCs to monitor transgene expression and function *in vitro* and *in vivo*. Expression of the GFP reporter molecule was well correlated with the expression of the C46 peptide (detected with the 2F5 monoclonal antibody) (Fig. 1b) and was also associated with a lower median fluorescence intensity (MFI) of CCR5 *in vitro* (Fig. 1c). Passive diffusion of the intrakine was ruled out by the observation that GFP⁺ cells exhibited similar CCR5 MFI than non-transduced cells (Fig. 1c), suggesting that this reduction was due to ER retention of CCR5 through interaction with the P2-CCL5 intrakine.. The MFI of CCR5 was also reduced two-fold in genetically-modified PBMCs injected *in vivo* in NSG mice (Fig. 1d), reflecting the expected down-modulation of CCR5 surface expression. Thus, GFP expression was a faithful reporter of transgenes expression and function, and was thus used to follow genetically-modified cells *in vivo*.

mice

As a model for HIV-1 infection of human CD4⁺ T cells *in vivo*, we first used adoptive cell transfer (ACT) in immunocompromised NSG mice (NSG/PBL). A major problem with ACT of human T cells in NSG mice is the xenogeneic graft-versus-host disease (GVHD) that develops thereafter and that invariably leads to death.²¹ We tested various ACT protocols in NSG mice and found that injection of 6.10⁶ activated T cells in 1 Gy-irradiated mice represented an optimal trade-off between survival and engraftment efficiency (protocol P3 in Figure S1). To normalize the number of genetically-modified cells across experiments and vectors, we diluted transduced cells into non-transduced cells *ex vivo* prior ACT, establishing a number of GFP⁺ cells at 10% of the injected cells. Mice were infected i.v with a CCR5-tropic HIV-1 strain 12 days after ACT. The frequencies of CD4⁺GFP⁺ cells steadily increased in the blood of LvGFP-C46-P2-treated animals during the course of the infection to reach a plateau where up to 95% of all CD4⁺ T cells expressed the transgene (Fig. 2a). In contrast, the frequencies of GFP⁺ cells in control HIV-1-infected LvGFP-treated mice remained close to the 10% input throughout the experiment (Fig. 2a). The increase in GFP⁺ cells with the LvGFP-C46-P2 vector was dependent on HIV-1 infection because it was not observed in non-infected NSG/PBL mice (Fig. S2), showing that the therapeutic vector did not increase the proliferation of modified cells *per se*. The frequencies of GFP⁺ cells were also superior in the spleen and in the bone marrow of LvGFP-C46-P2-treated mice compared with LvGFP-treated control mice (Fig. 2b). These increased frequencies translated into increased numbers of CD4⁺GFP⁺ cell in the spleen and the bone marrow of

LvGFP-C46-P2-treated mice compared with LvGFP mice (Fig. S3). Altogether, the results demonstrate that LvGFP-C46-P2-transduced CD4⁺ T cells possess a selective advantage relative to LvGFP-modified T cells.

To test the hypothesis that genetically-modified cells resisted HIV-1-induced depletion, we analyzed longitudinally the frequencies of CD4⁺ cells in CD3⁺GFP⁺ and CD3⁺GFP⁻ T cells in the blood of LvGFP-C46-P2- and LvGFP-treated mice (Fig. 2c). The frequencies of CD4⁺ T cells in the GFP⁻ subset rapidly dropped after HIV-1 infection, showing that non-protected CD4⁺ T cells underwent HIV-1-induced depletion as expected (Fig. 2d). In striking contrast, the frequency of CD4⁺ T cells in the GFP⁺ fraction remained constant throughout the experiment, showing that these cells were protected from HIV-1-induced depletion. Resistance to depletion was also observed in the spleen and in the bone marrow of LvGFP-C46-P2-treated animals, with statistically significant differences in the frequencies of CD4⁺ T cells in GFP⁺ vs GFP⁻ T cells (Fig. 2e). In contrast, the frequencies of GFP⁺ cells, like the GFP⁻ subset, steadily decreased in the blood of control LvGFP-treated mice (Fig. S4a), showing that GFP expression *per se* did not protect from HIV-1-induced deletion. A similar depletion of GFP⁺ cells were found in the spleen and in the bone marrow of control LvGFP-treated mice (Fig. S4b). Thus, CD4⁺ T cells expressing the combination of viral entry inhibitors were protected from HIV-1-induced depletion in NSG/PBL mice in the blood and in lymphoid tissues.

Resistance of genetically-modified human CD4⁺ T cells to HIV-1-induced depletion in NSG/CD34 HuMice

143 We next wanted to confirm the potency of the vector to prevent HIV-1-induced CD4⁺ T
144 cell depletion in a more physiological setting. For this, we grafted LvGFP-C46-P2-transduced
145 CD34-purified cells from cord blood into neonatal NSG mice and monitored human cell
146 reconstitution and transgene expression overtime. At 17 weeks post-injection, 11.9 ± 11.0 % of
147 total cells from the blood (excluding erythrocytes) were human CD45⁺CD3⁺ T cells in the
148 animals used for the experiment. The frequencies of CD4⁺ and CD8⁺ T cells among CD3⁺ cells
149 were less variable representing 40.0 ± 5.8 % and 47.0 ± 5.3 % , respectively (Fig. S5). Among 14
150 NSG/CD34 HuMice generated with LvGFP-C46-P2-modified CD34⁺ cells, only 8 had detectable
151 GFP⁺ cells in CD4⁺ T cells 17 weeks after. Four of those mice were infected with a CCR5-tropic
152 HIV-1 strain, whereas 4 were left uninfected. Because the frequency of GFP⁺ cells was highly
153 variable among NSG/CD34 HuMice, it was not possible to reliably measure a selective
154 advantage in that setting. To directly assess resistance of genetically-modified CD4⁺ T cells to
155 HIV-1-induced depletion, frequencies of CD4⁺ T cells were measured in GFP⁺ and GFP⁻ cells
156 (Fig. 3). In non-infected mice, the frequencies of CD4⁺ T cells in the blood remained similar in
157 GFP⁺ vs GFP⁻ T cells throughout the course of the experiment (Fig. 3a). As expected, frequencies
158 of GFP⁻ cells steadily decreased in HIV-1-infected animals whereas frequencies of GFP⁺
159 remained stable, showing that CD4⁺GFP⁺ T cells resisted HIV-1-induced depletion in the blood
160 of NSG/CD34 HuMice (Fig. 3b). As expected in non-infected mice, the frequencies of CD4⁺ T
161 cells in lymphoid organs were similar in GFP⁺ or GFP⁻ subsets (Fig. 3c). In contrast, frequencies
162 of CD4⁺ T cells among GFP⁺ and GFP⁻ cells significantly differed in the LN, spleen and bone
163 marrow (Fig. 3d). Of note is the one mouse in which resistance to deletion was not evident in the
164 blood did not show any sign of resistance in the lymphoid organs. Thus, gene transfer of two

entry inhibitors in CD34⁺ cells conferred resistance to CD4⁺ T cells in 3 mice out of 4 analyzed.

Gene transfer of entry inhibitors impact viral replication in NSG/CD34 HuMice.

To assess the impact that the therapy might have on viral loads, we measured viremia in LvGFP-C46-P2-treated mice in which GFP⁺ cells were observed (n=4) or not (n=6) prior HIV-1 infection. To accommodate the various levels of human cells engraftment among the different mice (Fig. S5), viremia was corrected by the frequency of CD45⁺CD3⁺CD4⁺ T cells among total cells of the blood at the time of the analysis. Initially, normalized viremia was similar in both groups, showing that the therapy was not associated with an immediate effect on viral replication. However, we observed a tendency for lower normalized viral loads in mice bearing GFP⁺ cells compared to mice in which no GFP⁺ cells could be detected (Fig. 4a). To confirm that animals with GFP⁺ cells carried less virus, we analyzed p24 expression in CD4⁺ T cells at the end of the experiment. We found that the frequencies of CD4⁺ cells expressing p24 in mice with GFP⁺ cells were lower than in mice without GFP⁺ cells and close to background staining obtained in non-infected HuMice (Fig. 4b). Altogether, we conclude that NSG/CD34 HuMice reconstituted with gene-modified CD34⁺ progenitors were protected from HIV-1-induced CD4⁺ T cell deletion and had a lower number of infected cells, corroborating with lower viral loads.

Discussion

Here, we show that a lentiviral vector encoding two viral entry inhibitors confers a selective advantage to genetically-modified cells *in vivo*, due to their resistance to HIV-1-mediated depletion. We observed a strong and long-lasting selective advantage in the NSG/PBL model. A lower selective advantage was reported in a very similar model of NSG/PBL HuMice using a vector expressing only the C46 peptide.¹⁸ This observation suggests that two entry inhibitors might be better than one at protecting cells from HIV-1. However, a pre-clinical study in macaques reconstituted with progenitors expressing the C46 peptide alone showed lower viral loads correlated to a clear selective advantage²². Moreover, recent studies showed that inhibition of CCR5 expression by shRNA was sufficient to protect CD4⁺ T cells from infection and to confer a selective advantage in chimeric Bone marrow-Liver-Thymus (BLT) HuMice^{23,24}. Thus, targeting gp41 and CCR5 have independently the potential to curb HIV-1 infection, highlighting the interest of using two inhibitors of this crucial step of HIV-1 infection in the same vector.

A strong selective advantage is not always associated with lower viral loads. In CD34-reconstituted HuMice, Walker et al. reported that expression of a triple combination of anti-HIV-1 genes did not impact viral replication, although a significant selective advantage was observed.²⁵ A modest but significant effect on viral loads was reported following CCR5-specific ZFN-mediated modification in NSG/PBL HuMice.⁵ However, only one time point was analyzed in that study. A kinetics study showed that the reduction in viral loads using the same technology was much more discrete in NSG/CD34 HuMice despite a considerable selective advantage.³ Our PCR and p24 data concur to the hypothesis that selective advantage conferred by our vector had

206 an impact on viral replication. Recently, a complete protection from HIV-1 was observed in BLT
207 mice reconstituted with human cells modified with a vector very similar to our, encoding the C46
208 peptide and a shRNA targeting CCR5¹⁹. This is the first report showing that viral replication can
209 be totally controlled in humanized mice by gene therapy without prior sorting of genetically-
210 modified cells, as recently shown for a CCR5 shRNA²⁶. This surprising and unique result
211 suggest that maximal efficacy of HIV-1 gene therapy might necessitate a functional immune
212 response, that is present in monkeys and BLT HuMice but lacking or severely hampered in other
213 HuMice models. One must keep in mind though that some HIV-1-specific PCR might amplify
214 the vector as well²⁷. The use of HIV-1-specific PCR discriminating HIV-1 from the vector such
215 as the one employed in our study should become the gold standard.

216 Considering the recent developments of nucleases that target CCR5 in CD34⁺ progenitor
217 cells, we believe that residual expression of the molecule such as the one observed with our
218 intrakine, might allow for normal hematopoiesis and circulation of modified-cells while total
219 ablation by genetic means may impact on these processes. Recent advances in lentiviral delivery
220 of ZN finger nucleases might improve specific targeting of the nuclease to mature CD4⁺ T cells, a
221 protocol that would limit bystander effects²⁸.

222 The selective advantage of genetically-modified cells would only be obtained in the
223 context of high levels of viral replication. Although ART interruptions have been performed in
224 the past to provoke selective growth of modified cells in small-scale clinical trials for gene
225 therapy,^{29,30} an interruption in therapy is not foreseeable in patients in the long term. Gene
226 therapy might thus be particularly suitable for patients experimenting treatment failure with high
227 viral loads.

228 **Materials and Methods**

229

230 *Lentiviral vector design and production*

231 Second-generation self-inactivating (SIN) lentiviral vectors were used in this study.³¹
232 The LvGFP-C46-P2 vector was constructed by adding an eGFP gene and 2A sequence upstream
233 of the therapeutic cassette (construction encoding the C46 peptide and P2-CCL5 analog
234 described in Petit et al., 2014)¹⁴ in the backbone of a lentiviral vector carrying the EF1a
235 promoter. As a control, the LvGFP vector expressing GFP only was used. Details on the cloning
236 procedures are available on request. Lentiviral vectors were produced in mycoplasma-free HEK-
237 293T cells, as described previously.³² Briefly, 23.3 µg of the Δ8.9 packaging plasmid, 30 µg of
238 the vector plasmid, and 10 µg of the vesicular stomatitis virus (VSV)-G envelope were
239 transfected into 15.10⁶ cells in T-175 flasks by calcium phosphate precipitation. Vector
240 supernatants were collected 48 hours post-transfection and concentrated by ultrafiltration
241 (Centricon Plus-70; Millipore, Molsheim, France) at 3500 g at 4°C. Viral stocks were kept frozen
242 at -80° C. Viral titers were determined on HEK-293T cells with various concentrations of vector
243 supernatants in the presence of Polybrene (8 µg/mL; Sigma-Aldrich, Saint-Quentin-Fallavier,
244 France). Seventy-two hours after transduction, the percentage of cells expressing the transgenes
245 was determined by flow cytometry and used to calculate a viral titer as the number of infectious
246 particles per milliliter.

247

248 *Mice and humanization*

249 NOD Prkdc^{scid} Il2rg^{tm1Wjl} (NSG) mice (strain #05557; Jackson Laboratory, USA) were
250 bred in animal facilities of Centre d'Expérimentation Fonctionnelle (CEF) according to the
251 Jackson Laboratory handling practice specific to that strain. The regional ethical committee on
252 animal experimentation Darwin approved all mouse protocols. Primary human cells were
253 obtained from leukapheresis samples collected from healthy donors at the Etablissement Français
254 du Sang after informed consent. Cells were grown at a concentration of 1.10^6 cells/mL and
255 activated in RPMI, 10% FCS, penicillin/streptomycin, interleukin-2 (Proleukin, 600 IU/mL;
256 Novartis, Basel, Switzerland), and CD3/CD28 beads (Invitrogen, Carlsbad, CA) at 3 beads per
257 cell. Two days after activation, cells were transduced by spinoculation for 2 hrs at 1000 g at
258 30°C, with the indicated lentiviral vectors at a multiplicity of infection (MOI) of 6 to 8 in the
259 presence of protamine sulfate (2 µg/mL, Sigma). Three days after transduction, 1 Gy-irradiated
260 female 8 to 12-weeks old NSG mice were injected with 6.10^6 cells. Twelve days post-adoptive
261 cell transfer (ACT), mice were infected with 25 ng of p24 of NLAD8 HIV-1 strain in a final
262 volume of 100 µL of 1X PBS. All mice used in this study were randomly assigned to
263 experimental group and cages. Investigator was not blinded to the group allocation during the
264 experiments.

265 Human hematopoietic progenitor cells were obtained from cord blood samples collected
266 from healthy donors after informed consent. Mononuclear cells from human cord blood were
267 isolated by Ficoll density gradient and centrifuged at 200 g during 13 min to remove platelets.
268 Then, CD34⁺ progenitors were sorted with the human CD34 MicroBeads kit, according to the
269 manufacturer's instructions (Miltenyi). CD34⁺ cells were incubated at a concentration of 1.10^6
270 cells/mL over night into StemSpan SFEMII medium (StemCell technologies) complemented with

human recombinant cytokines (IL-6 and TPO at 20 ng/mL; SCF and FLT3-L at 100 ng/mL; Peprotech) and antibiotics. Cells were transduced with the LvGFP-C46-P2 lentiviral vector in StemSpan medium in the presence of cytokines, the proteasome inhibitor MG-132 (1 μ M; Sigma), antibiotics and protamine sulfate (8 μ g/mL; Sigma). CD34⁺ cells underwent two rounds of transduction separated by 3 hours incubation at 37°C and 5% CO₂. For each transduction cycle, cells were centrifuged at 1000 g at 30°C for 2 hours with the lentiviral vector at a MOI of 15. Twenty-four to 48-hour-old NSG mice were irradiated at 0.9 Gy and grafted with 0.5.10⁵ to 2.5.10⁵ transduced CD34⁺ cells by the intra-hepatic route. Ten ng of the p24 NL-AD8 HIV-1 strain were injected into the retro-orbital sinus of 17 weeks-old mice in a final volume of 100 μ L of 1X PBS.

HIV-1 production and quantification

HIV-1 molecular clone NL-AD8 was obtained through the AIDS Research and Reference Reagent Program. HIV-1 stocks were prepared with 30 μ g of plasmid transfected into 15.10⁶ mycoplasma-free HEK 293T cells in T-175 flasks by calcium phosphate precipitation. The supernatant was frozen at -80°C and viral titers were quantified by p24 ELISA according to the manufacturer's instructions (Zeptometrix, Buffalo, NY). Mice were bled on ACD (acid-Citrate-Dextrose) anticoagulant and plasma HIV-1 RNA viral loads were measured using the Abbott RealTime HIV-1 RT-PCR assay that do not amplify genomic regions present in lentiviral vectors contrary to the Roche Cobas PCR (our unpublished observations and De Ravin et al ²⁷). Due to the small volumes of plasma from the mice, a dilution was necessary to reach the volume needed for the assay. Thus, this detection limit varied between 200 and 2000 copies/mL depending on the

293 initial volume of mouse plasma.

294

295 *Flow cytometry*

296 Red blood cells from whole blood were lysed with 4.5 ml of water for 15 s before adding
297 0.5 ml of 10X PBS. Red blood cells from spleen or bone marrow were lysed with ACK buffer
298 (NH_4Cl 0.15 M, KHCO_3 10 mM, EDTA 0.1 mM). Cell suspensions were stained with an optimal
299 quantity of antibodies at a concentration of 10^7 cells/mL in a final volume of 100 μL of PBS/FCS
300 3%. Incubation was performed in the dark at 6°C for 20 min. The following anti-human mAbs
301 were used for cell surface staining: CD45 PE-CF594 (clone HI30; catalog number (cat \neq)
302 562279, BD Biosciences) anti-CCR5 Alexa Fluor 647 (HEK/1/85a; cat \neq 313712, Biolegend),
303 anti-CD4 PerCP (RPA-T4, cat \neq 300528, Biolegend), anti-CD8 Alexa Fluor 700 (HIT8a, cat \neq
304 300920, Biolegend), CD3 PE-Cy7 (UCHT1, cat \neq 300420, Biolegend). The human IgG1 mAb
305 2F5 specific for a gp41 epitope (cat \neq AB001, Polymun, Austria) was used to detect the C46
306 peptide. The KC57-RD1 (cat \neq 6604667, Beckman Coulter) antibody was used to detect
307 intracellular p24 after cells were treated with permeabilization buffer (eBioscience, fixation and
308 permeabilization kit). All cell preparations were acquired on an LSRII cytometer (BD) and
309 analyzed with FlowJo software (Tree Star, Portland, OR). The frequencies of positive cells were
310 determined according to the fluorescence minus one (FMO) staining negative control.

311

312 *Statistical analysis*

313 No statistical method was used to assess sample size needed to detect an effect. Except for

314 the NSG/CD34 model, which is a single experiment, all the results shown in this study are
315 compiled from 2 independent experiments. Two-tailed p values indicated on the graphs were
316 calculated with Prism version 6.0 software (GraphPad Software, San Diego, CA), using the
317 unpaired Mann-Whitney test with a confidence interval of 95%. The median value are indicated
318 by horizontal bars on the graphs. Linear and non linear regression analysis were performed using
319 Prism 6.0 to determine whether slopes significantly differed. Plateau with one phase decay
320 association or dissociation equations were used to model the data.

321 **Acknowledgments**

322

323 This work was supported by grants from Agence Nationale de la Recherche to Guy Gorochov
324 and Gilles Marodon. Nicolas Petit was supported by a doctoral fellowship from Fond Pierre
325 Bergé /SIDAction and by the ANRS. The authors would like to thank David Klatzmann
326 (INSERM U959, Paris, France) for his initial support on this project, Dorothée van Laer
327 (Innsbruck University, Austria) for kind gift of the C46 peptide, Arnaud Moris (CIMI-PARIS,
328 France) for the kind gift of NL-AD8 HIV-1 strain, Dr Hans Yssel (CIMI-PARIS) for performing
329 Hoechst-based detection test of mycoplasma, Aude Burlion (CIMI-PARIS, France) for technical
330 help. Nicolas Petit, Claude Baillou and Gilles Marodon performed experiments; Béatrice
331 Levacher constructed the vectors; Corinne Amiel and Véronique Schneider performed HIV-1
332 qPCR; Karim Dorgham, Francois Lemoine, Guy Gorochov conceived experiments, contributed
333 to essential reagents and corrected the manuscript; Nicolas Petit and Gilles Marodon conceived
334 experiments, analyzed the data and wrote the manuscript.

335

336 **Conflict of Interest**

337 The authors declare no conflict of interest

338

339 Supplementary information is available at Gene Therapy's website

340

341 Figure S1. Survival and graft efficiency after ACT of activated and transduced T lymphocytes in
342 NSG/PBL HuMice.

343 Figure S2. Selective advantage for LvGFP-C46-P2-modified CD4⁺ cells is dependent on HIV-1
344 infection.

345 Figure S3. Resistance to HIV-1-induced deletion in LvGFP-C46-P2-injected NSG/PBL mice.

346 Figure S4. CD4⁺ T cell deletion in LvGFP-control NSG/PBL mice.

347 Figure S5. Human cell reconstitution in 17 weeks-old in NSG/CD34 humanized mice.

348

349

350

351 **References**

352

- 353 1 Martinson JJ, Chapman NH, Rees DC, Liu YT, Clegg JB. Global distribution of the CCR5 gene
354 32-basepair deletion. *Nat Genet* 1997; **16**: 100–103.
- 355 2 Allers K, Hütter G, Hofmann J, Loddenkemper C, Rieger K, Thiel E *et al*. Evidence for the cure
356 of HIV infection by CCR5 Δ 32/ Δ 32 stem cell transplantation. *Blood* 2011; **117**: 2791–9.
- 357 3 Holt N, Wang J, Kim K, Friedman G, Wang X, Taupin V *et al*. Human hematopoietic
358 stem/progenitor cells modified by zinc-finger nucleases targeted to CCR5 control HIV-1 in
359 vivo. *Nat Biotechnol* 2010; **28**: 839–847.
- 360 4 Didigu C a, Wilen CB, Wang J, Duong J, Secreto AJ, Danet-Desnoyers G a *et al*. Simultaneous
361 zinc-finger nuclease editing of the HIV coreceptors ccr5 and cxcr4 protects CD4+ T cells
362 from HIV-1 infection. *Blood* 2014; **123**: 61–9.
- 363 5 Perez EE, Wang J, Miller JC, Jouvenot Y, Kim KA, Liu O *et al*. Establishment of HIV-1
364 resistance in CD4+ T cells by genome editing using zinc-finger nucleases. *Nat Biotechnol*
365 2008; **26**: 808–816.
- 366 6 Tebas P, Stein D, Tang WW, Frank I, Wang SQ, Lee G *et al*. Gene Editing of CCR5 in
367 Autologous CD4 T Cells of Persons Infected with HIV. *N Engl J Med* 2014; **370**: 901–910.
- 368 7 Peterson CW, Younan P, Jerome KR, Kiem H-P. Combinatorial anti-HIV gene therapy: using a
369 multipronged approach to reach beyond HAART. *Gene Ther* 2013; **20**: 695–702.
- 370 8 Colin P, Bénureau Y, Staropoli I, Wang Y, Gonzalez N, Alcamí J *et al*. HIV-1 exploits CCR5
371 conformational heterogeneity to escape inhibition by chemokines. *Proc Natl Acad Sci U S*
372 A 2013; **110**: 9475–80.
- 373 9 Greenberg ML, Cammack N. Resistance to enfuvirtide, the first HIV fusion inhibitor. *J*
374 *Antimicrob Chemother* 2004; **54**: 333–340.
- 375 10 Von Laer D, Hasselmann S, Hasselmann K. Gene therapy for HIV infection: what does it need
376 to make it work? *J Gene Med* 2006; **8**: 658–667.
- 377 11 Doitsh G, Galloway NLK, Geng X, Yang Z, Monroe KM, Zepeda O *et al*. Cell death by
378 pyroptosis drives CD4 T-cell depletion in HIV-1 infection. *Nature* 2014; **505**: 509–14.
- 379 12 Heredia A, Gilliam B, DeVico A, Le N, Bamba D, Flinko R *et al*. CCR5 density levels on
380 primary CD4 T cells impact the replication and Enfuvirtide susceptibility of R5 HIV-1.
381 *Aids* 2007; **21**: 1317–1322.
- 382 13 Anastassopoulou CG, Ketas TJ, Sanders RW, Klasse PJ, Moore JP. Effects of sequence
383 changes in the HIV-1 gp41 fusion peptide on CCR5 inhibitor resistance. *Virology* 2012;
384 **428**: 86–97.
- 385 14 Petit N, Dorgham K, Levacher B, Burlion A, Gorochov G, Marodon G. Targeting Both Viral
386 and Host Determinants of Human Immunodeficiency Virus Entry, Using a New Lentiviral

387 Vector Coexpressing the T20 Fusion Inhibitor and a Selective CCL5 Intrakine. *Hum Gene*
388 *Ther Methods* 2014; **25**: 232–40.

389 15 Hartley O, Dorgham K, Perez-Bercoff D, Cerini F, Heimann A, Gaertner H *et al.* Human
390 immunodeficiency virus type 1 entry inhibitors selected on living cells from a library of
391 phage chemokines. *J Virol* 2003; **77**: 6637–6644.

392 16 Schroers R, Davis CM, Wagner HJ, Chen SY. Lentiviral transduction of human T-
393 lymphocytes with a RANTES intrakine inhibits human immunodeficiency virus type 1
394 infection. *Gene Ther* 2002; **9**: 889–897.

395 17 Egelhofer M, Brandenburg G, Martinius H, Schult-Dietrich P, Melikyan G, Kunert R *et al.*
396 Inhibition of Human Immunodeficiency Virus Type 1 Entry in Cells Expressing gp41-
397 Derived Peptides. *J Virol* 2004; **78**: 568–575.

398 18 Kimpel J, Braun SE, Qiu G, Wong FE, Conolle M, Schmitz JE *et al.* Survival of the Fittest:
399 Positive Selection of CD4+ T Cells Expressing a Membrane-Bound Fusion Inhibitor
400 Following HIV-1 Infection. *PLoS One* 2010; **5**: e12357.

401 19 Burke BP, Levin BR, Zhang J, Sahakyan A, Boyer J, Carroll M V *et al.* Engineering Cellular
402 Resistance to HIV-1 Infection In Vivo Using a Dual Therapeutic Lentiviral Vector. *Mol*
403 *Ther Acids* 2015; **4**: e236.

404 20 Trobridge GD, Wu RA, Beard BC, Chiu SY, Muñoz NM, von Laer D *et al.* Protection of stem
405 cell-derived lymphocytes in a primate AIDS gene therapy model after in vivo selection.
406 *PLoS One* 2009; **4**. doi:10.1371/journal.pone.0007693.

407 21 King MA, Covassin L, Brehm MA, Racki W, Pearson T, Leif J *et al.* Human peripheral blood
408 leucocyte non-obese diabetic-severe combined immunodeficiency interleukin-2 receptor
409 gamma chain gene mouse model of xenogeneic graft-versus-host-like disease and the role
410 of host major histocompatibility complex. *Clin Exp Immunol* 2009; **157**: 104–118.

411 22 Younan PM, Polacino P, Kowalski JP, Peterson CW, Maurice NJ, Williams NP *et al.* Positive
412 selection of mC46-expressing CD4+ T cells and maintenance of virus specific immunity in
413 a primate AIDS model. *Blood* 2013; **122**: 179–187.

414 23 Shimizu S, Ringpis G-E, Marsden MD, Cortado R V, Wilhalme HM, Elashoff D *et al.* RNAi-
415 Mediated CCR5 Knockdown Provides HIV-1 Resistance to Memory T Cells in Humanized
416 BLT Mice. *Mol Ther Nucleic Acids* 2015; **4**: e227.

417 24 Myburgh R, Ivic S, Pepper MS, Gers-Huber G, Li D, Audigé A *et al.* Lentivector knock-down
418 of CCR5 in hematopoietic stem cells confers functional and persistent HIV-1 resistance in
419 humanized mice. *J Virol* 2015; **89**: 6761–6772.

420 25 Walker JE, Chen RX, McGee J, Nacey C, Pollard RB, Abedi M *et al.* Generation of an HIV-1-
421 Resistant Immune System with CD34+ Hematopoietic Stem Cells Transduced with a
422 Triple-Combination Anti-HIV Lentiviral Vector. *J. Virol.* 2012; **86**: 5719–5729.

423 26 Myburgh R, Ivic S, Pepper MS, Gers-Huber G, Li D, Audigé A *et al.* Lentivector knock-down
424 of CCR5 in hematopoietic stem cells confers functional and persistent HIV-1 resistance in
425 humanized mice. *J Virol* 2015; **89**: 6761–6772.

426 27 De Ravin SS, Gray JT, Throm RE, Spindler J, Kearney M, Wu X *et al.* False-Positive HIV
427 PCR Test Following Ex Vivo Lentiviral Gene Transfer Treatment of X-linked Severe
428 Combined Immunodeficiency Vector. *Mol Ther* 2014; **22**: 244–245.

429 28 Abarrategui-Pontes C, Cr  neguy A, Thinard R, Fine EJ, Thepenier V, Fournier LRL *et al.*
430 Codon swapping of zinc finger nucleases confers expression in primary cells and in vivo
431 from a single lentiviral vector. *Curr Gene Ther* 2014; **14**: 365–76.

432 29 DiGiusto DL, Krishnan A, Li L, Li H, Li S, Rao A *et al.* RNA-based gene therapy for HIV
433 with lentiviral vector-modified CD34(+) cells in patients undergoing transplantation for
434 AIDS-related lymphoma. *Sci Transl Med* 2010; **2**: 36ra43.

435 30 Podsakoff GM, Engel BC, Carbonaro DA, Choi C, Smogorzewska EM, Bauer G *et al.*
436 Selective survival of peripheral blood lymphocytes in children with HIV-1 following
437 delivery of an anti-HIV gene to bone marrow CD34+ cells. *Mol Ther* 2005; **12**: 77–86.

438 31 Zufferey R, Dull T, Mandel RJ, Bukovsky A, Quiroz D, Naldini L *et al.* Self-inactivating
439 lentivirus vector for safe and efficient in vivo gene delivery. *J Virol* 1998; **98**: 9873–9880.

440 32 Marodon G, Mouly E, Blair EJ, Frisen C, Lemoine FM, Klatzmann D. Specific transgene
441 expression in human and mouse CD4+ cells using lentiviral vectors with regulatory
442 sequences from the CD4 gene. *Blood* 2003; **101**: 3416–3423.

443

Figure Legends

Figure 1. Lentiviral vector design and co-expression of anti-HIV-1 genes and eGFP into a lentiviral vector. (a) A schematic representation of the structure of the lentiviral vectors used in the present study is shown. (LTR: long terminal repeat; cypT: central polypurine tract of HIV-1; EF1 α : Elongation factor 1 promoter; C46: membrane-bound form of T20 (C46 peptide); 2A: 2A sequence of the foot-and-mouth disease virus; P2i: P2-CCL5 intrakine; WPRE: Woodchuck Hepatitis virus regulatory element; Δ LTR: U3 deleted LTR). Indicated is the reference of the vector used throughout the study. Not to scale. (b) Co-expression of the C46 peptide (detected with the 2F5 mAb) and of eGFP and (c) co-expression of CCR5 and eGFP in human CD4⁺ PBMC activated by CD3/CD28 beads and IL-2 21 to 29 days post transduction with the LvGFP-C46-P2 vector (NT: Non-transduced; FMO: fluorescence minus one; MFI: median fluorescence intensity) (d) *In vivo* CCR5 expression on CD45⁺CD3⁺CD4⁺ T cells in GFP⁺ and GFP⁻ cells from non-irradiated NSG mice grafted with 2.10⁶ LvGFP-C46-P2 transduced T lymphocytes and analyzed in the blood and the spleen 34 to 53 days post-graft.

Figure 2. Protection of genetically-modified human CD4⁺ T cells from HIV-1 infection in NSG/PBL mice. (a-b) Frequencies of GFP⁺ cells in human CD45⁺CD3⁺CD4⁺ T cells in the blood at various days after HIV-1 infection (a) and in the spleen or bone marrow (BM) (b) 35 to 45 days after injection of LvGFP- or LvGFP-C46-P2-modified T cells in NSG mice. (c) Representative histograms and dot plots showing the gating strategy to determine the frequencies of CD4⁺ T cells in GFP⁺ and GFP⁻ human CD3⁺ T cells. (d-e) Frequencies of CD4⁺ cells in the CD3⁺GFP⁺ and CD3⁺GFP⁻ populations were determined in LvGFP-C46-P2-injected mice in the blood at various days after infection (d) and in the spleen or bone marrow (BM) (e) at the end of the experiment. The results are compiled from 2 independent experiments using the P3 ACT protocol (Fig. S1). Non linear regression analysis curve fit are shown. The p value indicate the significant difference between the two slopes.

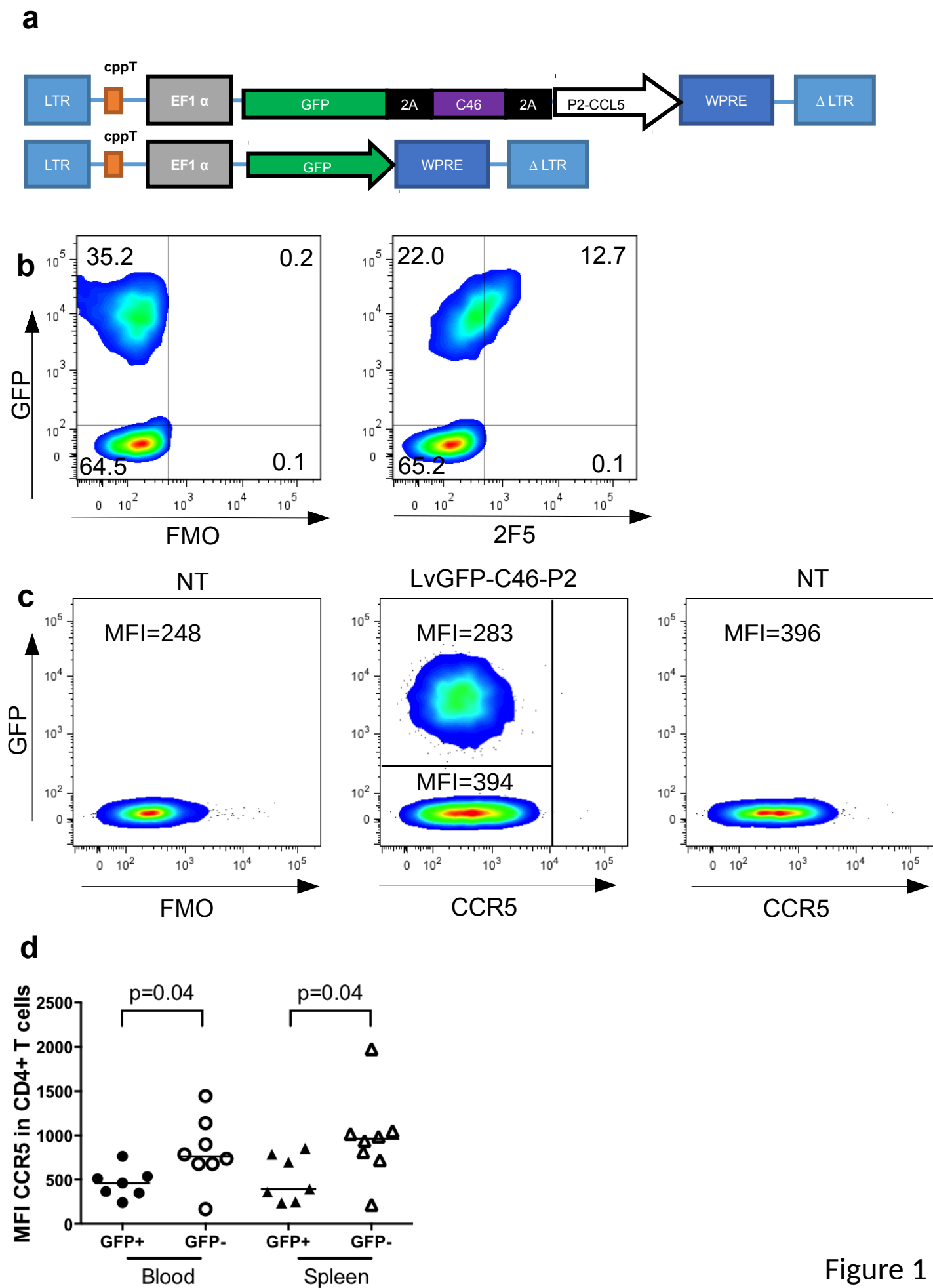
Figure 3. Resistance of genetically-modified CD4⁺ T cells to HIV-1-induced depletion *in vivo* in NSG/CD34 HuMice. (a) Blood frequencies of CD4⁺ cells in CD3⁺GFP⁺ or CD3⁺GFP⁻

473 populations were determined in non-infected (HIV⁻) or **(b)** infected (HIV⁺) NSG HuMice at
474 various time points after infection. Linear regression curve fit and p values are depicted on the
475 graphs. n.s = not significant (p>0.05) **(c)** Frequencies of CD4⁺ cells into CD3⁺GFP⁺ or
476 CD3⁺GFP⁻ populations in HIV⁻ or **(d)** HIV⁺ mice in the spleen, the lymph nodes (LN) and the
477 bone marrow (BM) 11 weeks post-infection.

478

479 **Figure 4. Gene transfer of entry inhibitors impacts viral replication in NSG/CD34 HuMice**

480 **(a)** Viral load was measured by qPCR after HIV-1 infection in LvGFP-C46-P2-treated mice with
481 undetectable (-GFP) or detectable GFP⁺ cells (+GFP) in CD4⁺ T cells prior to infection. Shown is
482 the viral load value normalized by the frequency of human CD45⁺CD3⁺CD4⁺ T cells present in
483 total cells of the blood sample for each time point. **(b)** Frequencies of p24⁺ cells in CD4⁺ T cells
484 from the lymph node of NSG HuMice with (+GFP) or without GFP⁺ cells (-GFP) 77 days after
485 infection with NL-AD8 HIV-1 (HIV⁺) or non infected (HIV⁻). A representative CD4 vs p24
486 staining is shown above each group. One mouse from the (+GFP) group was excluded from the
487 graph since it did not show any protection against HIV-1-induced depletion in the periphery.



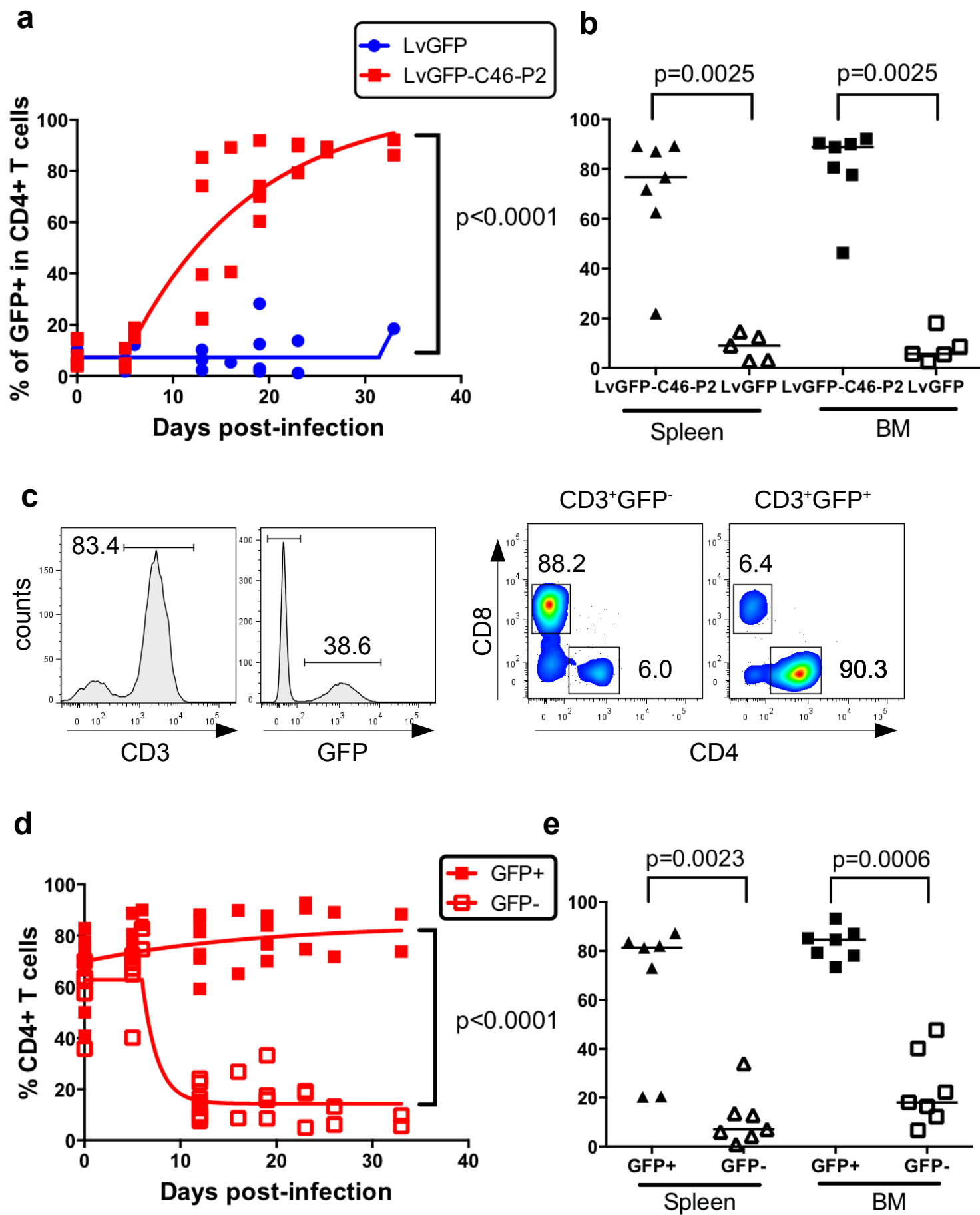


Figure 2

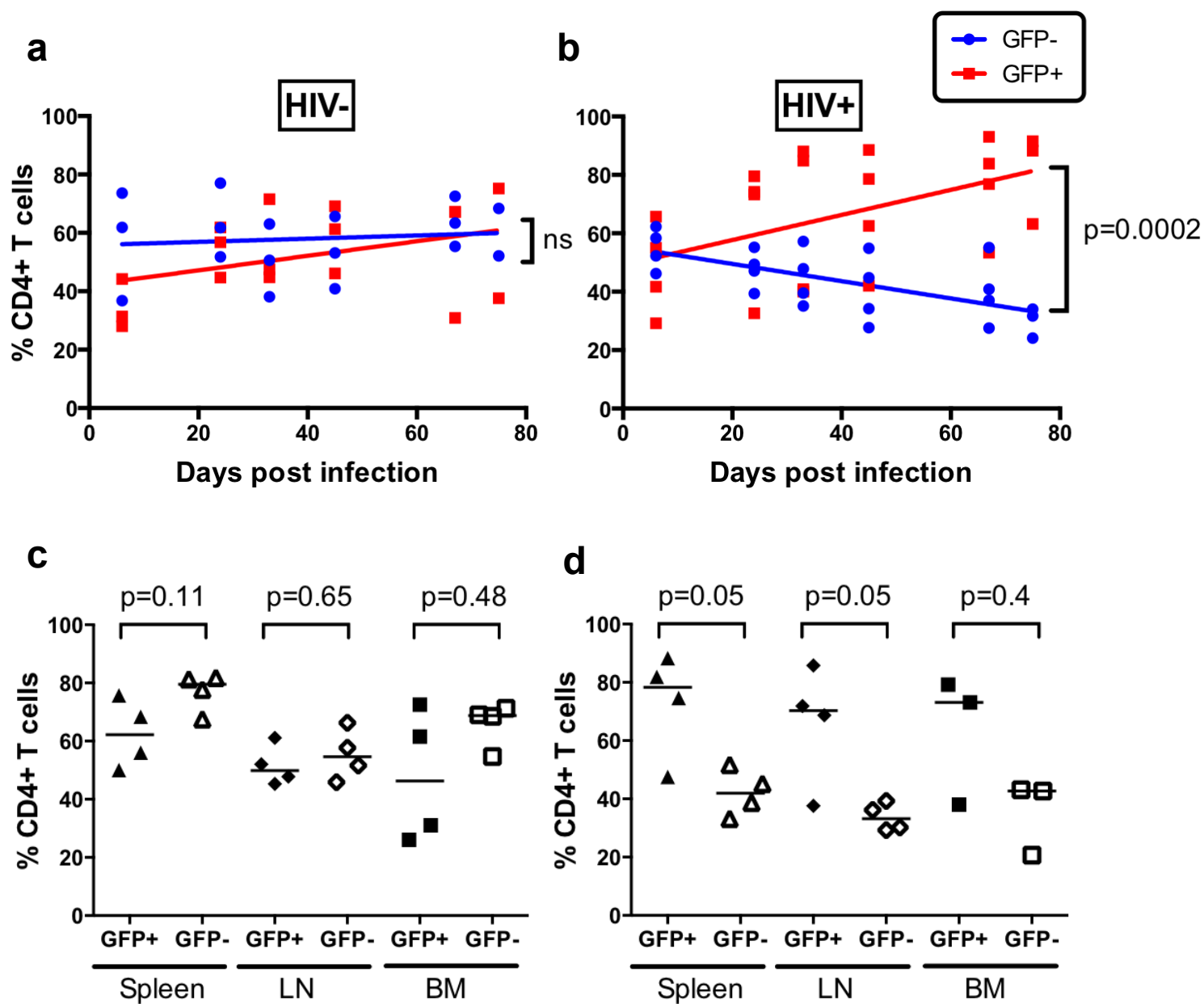


Figure 3

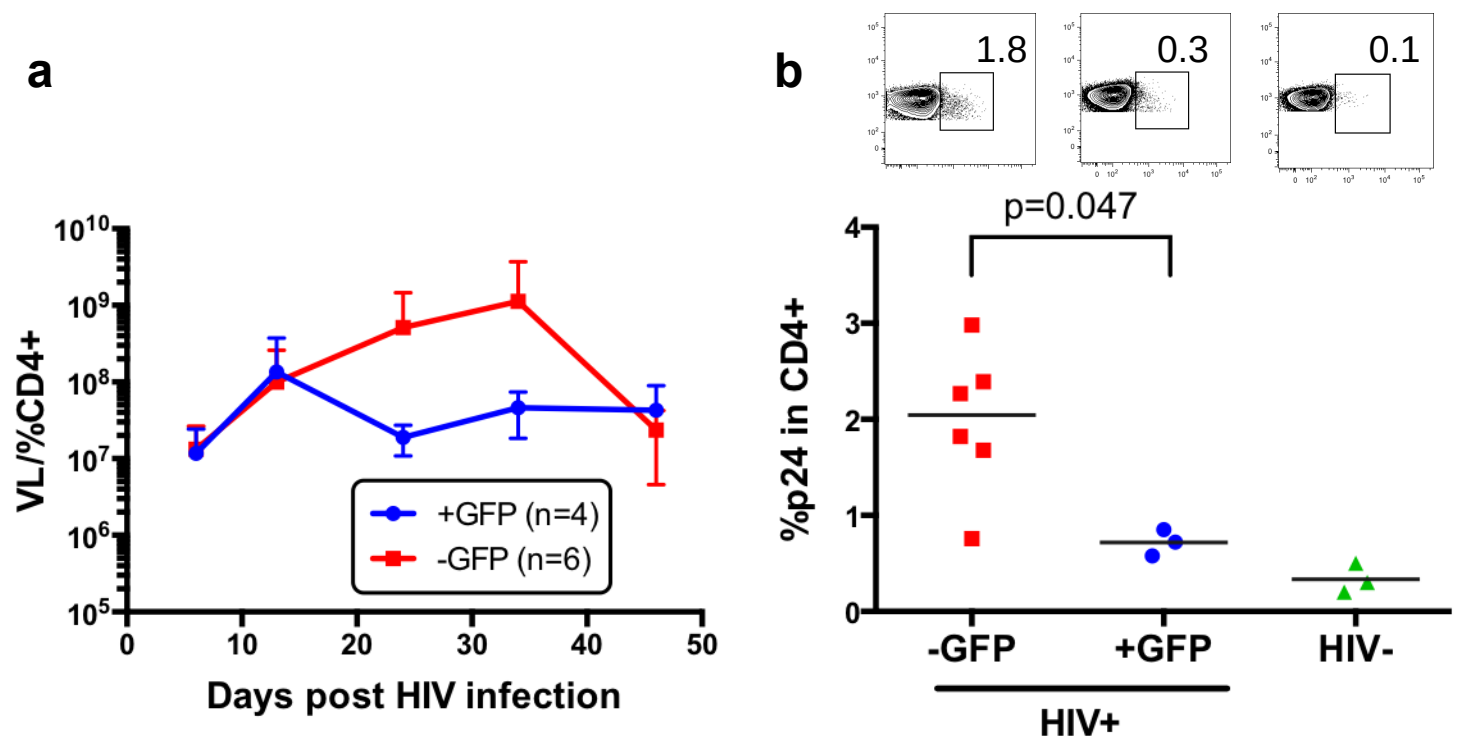


Figure 4